Enthalpic and entropic contributions to the activation free energy of single noncovalent bonds in molecular systems: A computational methodology

Jakub Dąbrowski,[1] Wieslaw Nowak,[2] and Arkadiusz Ptak[1,*]
[1]*Institute of Physics, Faculty of Materials Engineering and Technical Physics, Poznan University of Technology, Piotrowo 3, PL-60965 Poznan, Poland*
[2]*Institute of Physics, Faculty of Physics, Astronomy and Informatics, Nicolaus Copernicus University, Grudziadzka 5, PL-87100 Torun, Poland*

(Received 9 June 2022; accepted 17 November 2022; published 2 December 2022)

Insight into enthalpic and entropic contributions to the activation free energy of noncovalent bonds is crucial for understanding various phenomena in molecular systems, from formation of different molecular conformers to complex biophysical and biochemical processes. Standard experimental and computational methods provide only the average strength of noncovalent bonds. In this paper, we present a simple, formal, computational framework to determine both energy contributions for a single bond. Our approach is based on steered molecular dynamics simulations, the dynamic force spectroscopy method, and a modified theoretical model of force-induced bond rupture. To demonstrate the methodology, the enthalpic and entropic components for a single intramolecular hydrogen bond of a peptide helix were determined. The sum of the contributions is in agreement with the previously reported Gibbs energy for intramolecular hydrogen bonds. The proposed methodological framework is universal and can be applied to other noncovalent interactions in various molecular systems.

DOI: 10.1103/PhysRevA.106.062803

I. INTRODUCTION

From the point of view of thermodynamics, bond formation is driven by minimization of the Gibbs free energy, while unbinding occurs when a sufficient amount of energy is delivered to the bond. However, in numerous processes, such as solvation, complexation, phase coexistence, or binding affinity, different mechanisms can be characterized by similar change in the Gibbs free energy, whereas their enthalpy and entropy contributions are fundamentally different [1–4]. Therefore, insight into the energy components allows a better understanding of the molecular processes. In particular, the knowledge on enthalpic and entropic contributions is crucial for understanding the mechanisms of formation and rupture of noncovalent bonds, which govern more complex processes—from the formation of various conformers of simple molecules [5] to multistage biophysical and biochemical processes, such as protein folding or ligand-receptor bindings [6–8].

The commonly used experimental methods like circular dichroism, microcalorimetry, or NMR spectroscopy do not provide microscopic information about the Gibbs energy (and its components) of single noncovalent bonds [2,8]. Such information can be provided by computational methods, although they are usually characterized by high uncertainty. This is due to the fact that the values of Gibbs energy are very large compared to their changes accompanying the formation and breaking of noncovalent bonds. Among the most commonly used computational methods are those based on free-energy perturbation [3] and integration thermodynamics methods [4]. Such an approach allows obtaining information about the average changes in the Gibbs energy and its components accompanying molecular processes, but without analyzing individual events, such as the rupture of a noncovalent intramolecular bond.

The methodology we propose leads to the information about the thermodynamics, and additionally the kinetics of a single noncovalent bond rupture. The procedure includes steered molecular dynamics (SMD) simulations [9], the application of the dynamic force spectroscopy (DFS) [10] method, and a modification of a theoretical model of force-induced bond rupture. To illustrate the methodology, an α-helical peptide stabilized by intramolecular hydrogen bonds (HBs), with the AEAAKA (A: alanine; E: glutamic acid; K: lysine) sequence motif commonly found in transmembrane proteins, was used as a model molecule. In such a peptide the controlled unfolding of the helix is accompanied by the rupture (unbinding) of backbone HBs.

II. METHODS

A. Peptide model preparation and computational protocol

The AAKA$(AEAAKA)_5$-AC model (C: cysteine) was assembled in predefined α-helical conformation using VMD software [11]. This amino acid sequence was chosen for its high α-helical propensity leading to a stable α-helical conformation during simulations [12]. The NAMD 2.13 package [13] with the implemented CHARMM36 force field [14,15] was used to perform geometry optimization (energy minimization), heating, molecular dynamics (MD), and SMD simulations (Fig. 1).

*Corresponding author: arkadiusz.ptak@put.poznan.pl

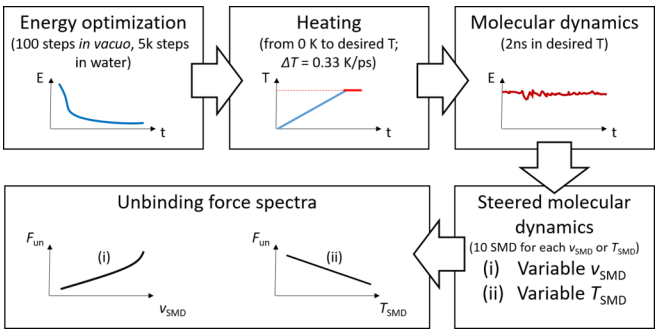

FIG. 1. A scheme of the computational protocol. After the energy minimization and heating simulations, 2 ns MD simulation was performed, and ten system configurations with the highest α-helix content were selected as starting points for successive SMD simulations for different SMD velocities (v_{SMD}) and different SMD temperatures (T_{SMD}).

In the SMD simulations a harmonic potential ($k_{SMD} = 16.75\,\mathrm{kJ\,mol^{-1}\,\AA^{-2}}$) was applied to the sulfur atom in the C-terminal cysteine, whereas the C_α atom of the third residue ($K3$) was fixed in space (Fig. 2). The pulling vector reflected the direction of the force applied in atomic force spectroscopy experiments [16,17]. No barostats nor thermostats were used for SMD simulations to avoid their possible influence on the results, in particular artifacts such as abrupt deformations of the α-helix and hence accidental crossing of HB activation barriers or the HB length criterion. Details on the simulation protocol can be found in the Supplemental Material [18].

B. Theoretical model of force-induced unbinding

In our approach we assume that the mechanical rupture of a HB can be treated as a thermally activated and force-facilitated escape from a one-dimensional potential well [19]. Several theoretical models, based on this assumption, provide the formula for the dependence of the unfolding force on the loading rate. The most common, applied widely in the studies of intra- and intermolecular interactions, is the Bell-Evans model [10,20]. However, this model has several disadvantages, including the most significant one: The whole information about the shape of the interaction potential describing a bond is reduced to a single parameter—the position of the activation barrier with respect to the bound state minimum. Therefore, we decided to apply in the present framework the more advanced Dudko-Hummer-Szabo (DHS) model [21]. The DHS model delivers the following formula for the most probable unbinding force:

$$F_{\mathrm{un}} = \frac{\Delta G_\beta}{\nu x_\beta}\left\{1 - \left[\frac{k_{\mathrm{B}}T}{\Delta G_\beta}\ln\frac{k_{\mathrm{off}}^0 k_{\mathrm{B}}T\exp\left(\frac{\Delta G_\beta}{k_{\mathrm{B}}T}\right)}{x_\beta r_{\mathrm{F}}}\right]^{\nu}\right\}, \quad (1)$$

where ΔG_β is the Gibbs free energy of activation in the absence of external forces, k_{off}^0 is the force-free unbinding rate, x_β is the distance between the bound state minimum and the maximum of the activation barrier in the one-dimensional (in the direction of the applied force) free-energy potential, $r_F \equiv dF/dt$ is the loading rate, k_{B} is the Boltzmann constant, T is the absolute temperature, and the parameter ν is related to the shape of the free-energy potential. Dudko *et al.* [21] have suggested to use $\nu = 2/3$ as a universal value in their model, for the Lennard-Jones type potentials as well. The DHS model, besides its higher accuracy, has another advantage over the Bell-Evans model; it enables extraction of ΔG_β in addition to k_{off}^0 and x_β.

III. RESULTS AND DISCUSSION

A. Force curves and unbinding force

As a result of the SMD simulations, force-versus-elongation curves were obtained (Fig. 3). Peaks observed in the force curve indicate HB rupture events. In our previous paper [19] we have shown that the most probable number of HBs broken in the first rupture event (first peak) is 1, for all applied loading rates. Here, we show that only a single HB which breaks is significantly elongated before the rupture point (Fig. S5 in the Supplemental Material [18]). Therefore, the unbinding force of a single HB (F_{un}) was extracted from the first peak for each force-elongation curve (Fig. 3). The procedure for determining the first peak as a local maximum is described in detail in the Supplemental Material [18].

B. Dynamic force spectra and their interpretation

We performed two sets of SMD simulations: (i) at a constant temperature $T = 300$ K for eight different SMD velocities (v_{SMD}) : 0.3, 0.5, 0.75, 1, 1.5, 2, 4, and 5 $\mathrm{\AA\,ps^{-1}}$; and (ii) at a constant $v_{SMD} = 1\,\mathrm{\AA\,ps^{-1}}$ for nine different temperatures (T_{SMD}) from 270 to 310 K, in 5 K steps. For each value of v_{SMD} and T_{SMD}, ten SMD simulations were performed. Ten extracted values of F_{un} were collected into a histogram and the most probable value of F_{un} was determined from the lognormal distribution function fitted to the histogram. The lognormal function was found to more accurately

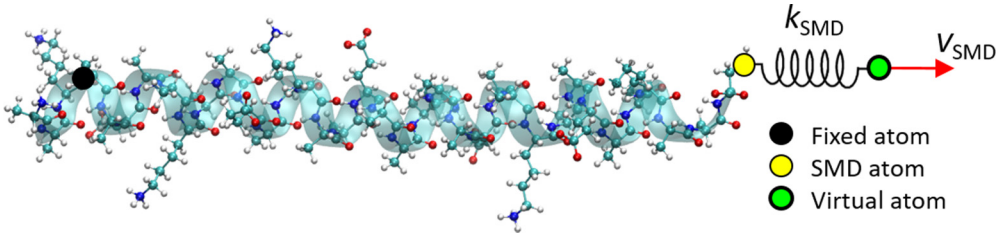

FIG. 2. A schematic representation of the SMD simulation. The peptide model is in the initial conformation; solvent molecules are not presented; k_{SMD} is the SMD spring constant and v_{SMD} is the virtual atom velocity (SMD velocity).

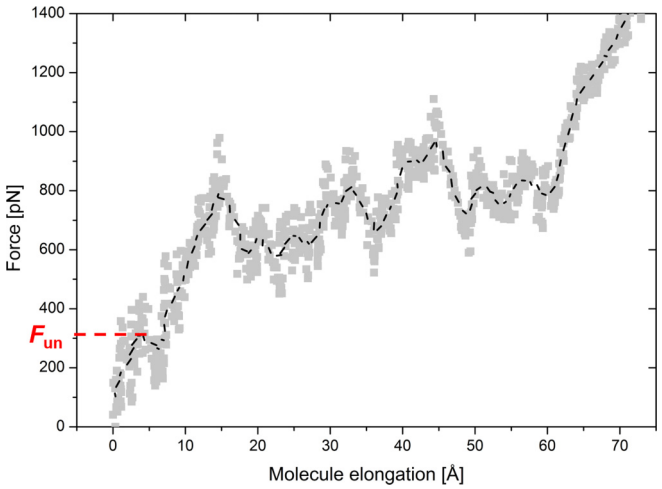

FIG. 3. An example of the force-elongation dependence (gray squares). The data were analyzed with the FFT smooth filter (dashed black line). The unbinding force (F_{un}) of a HB rupture in the α-helix was determined from the first peak (a local maximum) of the smoothed force-elongation plot. The data were recorded at the pulling velocity of 0.75 Å ps^{-1} at the simulation temperature of 300 K.

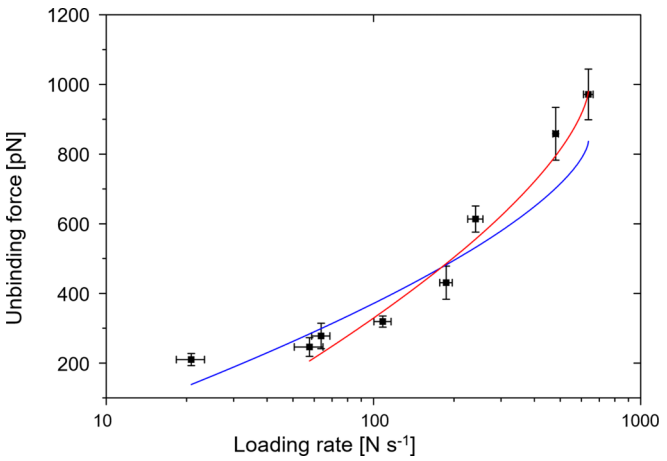

FIG. 4. The most probable unbinding force as a function of the loading rate. The data are fitted with the DHS model for two loading rate ranges: whole (21–626 N s^{-1}, blue line), and limited (57–626 N s^{-1}, red line). The error bars show standard errors.

describe such asymmetrical data distributions than the widely used Gaussian function. The F_{un} distribution is asymmetrical as a rule; the left tail of the distribution is limited by zero, since the unbinding force cannot be negative, whereas the right tail is, at least in principle, unlimited (Fig. S6 in the Supplemental Material [18]).

The most probable values of F_{un} are presented as a function of the loading rate, i.e., the increment of the applied force in time (N/s), which gives the so-called dynamic force spectrum in Fig. 4.

We fitted the DHS model to two ranges of the simulated dynamic force spectrum of the model peptide: the whole range of loading rates (21–626 N s^{-1}, blue curve in Fig. 4) and the limited range, i.e., without the lowest value of the loading rate (57–626 N s^{-1}, red curve in Fig. 4). The fitting for the limited range is much better than for the whole range: $R^2_{adj} = 0.92$ versus $R^2_{adj} = 0.75$ (Table I). We associate this fact with the process of HB re-formation (rebinding), which is more probable at lower loading rates. Since the DHS model does not take into account the rebinding, it is more effective for higher loading rates, where the probability of rebinding is low. Therefore, cutting from the fitting range the low loading rates improves the quality of fitting. Further limitation of the fitting range, above 57 N s^{-1}, does not change the fitting results significantly; therefore, in further analysis we used the fitting parameters obtained for the range of 57–626 N s^{-1}.

The determined value of $\Delta G_\beta = (8.5 \pm 0.9)$ kJ mol^{-1} is lower than that obtained earlier [19], which we attribute mainly to a wider range of loading rates in the previous simulations and, thus, to a higher contribution of the rebinding, which is eliminated in our present study. The present value, however, is in good agreement with experimental values [22] as well as the energy reported by Sheu *at al.* [23] for a HB in a helical peptide in water (8.1 kJ mol^{-1}).

C. Enthalpic and entropic contributions

The Gibbs free energy has enthalpic and entropic components:

$$\Delta G_\beta = \Delta H - T\Delta S. \tag{2}$$

Substitution of the above formula into Eq. (1) leads to the following formula for the temperature-dependent unbinding force:

$$F_{un}(T) = \frac{\Delta H - T\Delta S}{\nu x_\beta}\left\{1 - \left[\frac{k_B T}{\Delta H - T\Delta S}\ln\left(\frac{k_B T}{x_\beta \tau_D r_F}\right)\right]^\nu\right\}, \tag{3}$$

TABLE I. Fitting parameters obtained with the DHS model for the most probable unbinding force versus the loading rate $F_{un}(r_F)$.

Loading rate range (N s^{-1})	x_β[a] (Å)	ΔG_β[b] (kJ mol^{-1})	k^0_{off}[c] (10^{10} s^{-1})	R^2_{adj}[d]
21–626	0.33 ± 0.06	10.9 ± 4.6	6.1 ± 1.6	0.75
57–626	0.22 ± 0.04	8.54 ± 0.88	10.9 ± 1.5	0.92

[a] x_β is the distance between the HB bound state minimum and the position of the activation barrier.
[b] ΔG_β is the Gibbs free energy of activation in the absence of the external force.
[c] k^0_{off} is the force-free unbinding rate.
[d] R^2_{adj} is the adjusted coefficient of determination.

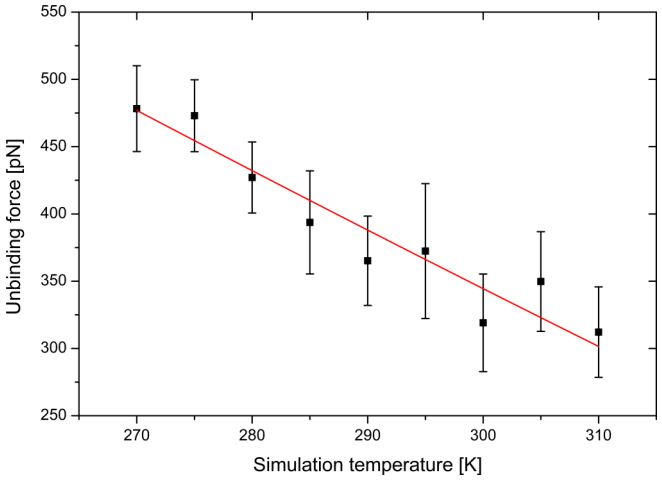

FIG. 5. The most probable unbinding force as a function of the simulation temperature (T_{SMD}). The data are fitted with the modified DHS model (red line). The error bars show standard errors.

where τ_{D} is the characteristic diffusion time of motion in the system calculated as

$$\tau_{\mathrm{D}} = \frac{1}{k_{\mathrm{off}}^{0}} \exp\left(-\frac{\Delta G_{\beta}}{k_{\mathrm{B}} T}\right). \tag{4}$$

By calculating x_{β}, ΔG_{β}, and k_{off}^{0} from the $F_{\mathrm{un}}(v_{\mathrm{SMD}})$ dependence [Eq. (1)] and then fitting the modified DHS model [Eq. (3)] to the $F_{\mathrm{un}}(T_{\mathrm{SMD}})$ dependence determined from the second SMD simulation set (Fig. 5), the enthalpic ΔH and entropic $T\Delta S$ components of the Gibbs free energy of activation can be extracted (Table II).

The sum of the enthalpic and entropic components, $\Delta H – T\Delta S = 8.6\,\mathrm{kJ\,mol^{-1}}$, is in agreement with the ΔG_{β} obtained by fitting Eq. (1) to the $F_{\mathrm{un}}(v_{\mathrm{SMD}})$ dependence. The atoms involved in the HB (as well as the part of the backbone between them) gain some freedom after a rupture event and therefore the entropic component lowers the HB activation energy barrier. This is consistent with the total conformational entropic energy per residue at 300 K ($5.9\,\mathrm{kJ\,mol^{-1}}$) calculated for ubiquitin (protein) folding [24].

TABLE II. Enthalpic (ΔH) and entropic ($\mathrm{T}\Delta S$) contributions to the Gibbs free energy of activation obtained by fitting Eq. (3) to the $F_{\mathrm{un}}(T_{\mathrm{SMD}})$ dependence.

$\Delta H\,(\mathrm{kJ\,mol^{-1}})$	$\mathrm{T}\Delta S\,(\mathrm{kJ\,mol^{-1}})$ for 300 K	R^2_{adj} [a]
15.4 ± 1.5	6.9 ± 1.6	0.91

[a] R^2_{adj} is the adjusted coefficient of determination.

IV. CONCLUSIONS

A combination of two simulation sets, $F_{\mathrm{un}}(v_{\mathrm{SMD}})$ and $F_{\mathrm{un}}(T_{\mathrm{SMD}})$, and the proposed modification of the DHS model provide a framework for obtaining quantitative information about enthalpic and entropic contributions to the activation free energy of a single noncovalent bond. The knowledge of these contributions is necessary to understand the behavior of molecular systems, including conformational changes of molecules and the folding and unfolding of proteins and nucleic acids, as well as specific ligand-receptor affinity. The proposed computational methodology is universal and can be applied to various types of intra- or intermolecular interactions, enriching and accelerating studies of numerous molecular processes. Similar methodology can also be used to analyze experimental data obtained using an atomic force microscope (AFM) or other device operating in the so-called force spectroscopy mode. However, controlling the process of unbinding in AFM (or similar) force spectroscopy experiments is much more difficult than in molecular simulations.

ACKNOWLEDGMENT

This work was supported by the Ministry of Education and Science in Poland under Project No. 0512/SBAD/2120 realized at the Faculty of Materials Engineering and Technical Physics, Poznan University of Technology.

[1] G. S. Ratnaparkhi and R. Varadarajan, Thermodynamic and structural studies of cavity formation in proteins suggest that loss of packing interactions rather than the hydrophobic effect dominates the observed energetics, Biochemistry **39**, 12365 (2000).

[2] F. Perret, J. P. Morel, and N. Morel-Desrosiers, Thermodynamics of the complexation of the *p*-sulfonatocalix [4] arene with simple model guests in water: A microcalorimetric study, Supramol. Chem. **15**, 199 (2003).

[3] N. Lu, D. A. Kofke, and T. B. Woolf, Staging is more important than perturbation method for computation of enthalpy and entropy changes in complex systems, J. Phys. Chem. B **107**, 5598 (2003).

[4] A. Ghoufi and P. Malfreyt, Entropy and enthalpy calculations from perturbation and integration thermodynamics methods using molecular dynamics simulations: Applications to the calculation of hydration and association thermodynamic properties, Mol. Phys. **104**, 2929 (2006).

[5] R. Siewert, K. V. Zherikova, and S. P. Verevkin, Non-covalent interactions in molecular systems: Thermodynamic evaluation of the hydrogen-bond strength in amino-ethers and amino-alcohols, Chem. - Eur. J. **28**, e202200080 (2022).

[6] L. Liu, C. Yang, and Q. X. Guo, A Study on the enthalpy-entropy compensation in protein unfolding, Biophys. Chem. **84**, 239 (2000).

[7] A. Bastida, J. Zúñiga, A. Requena, B. Miguel, and J. Cerezo, On the role of entropy in the stabilization of α-helices, J. Chem. Inf. Model. **60**, 6523 (2020).

[8] M. Dreydoppel, J. Balbach, and U. Weininger, Monitoring protein unfolding transitions by NMR-spectroscopy, J. Biomol. NMR **76**, 3 (2022).

[9] S. Izrailev, S. Stepaniants, B. Isralewitz, D. Kosztin, H. Lu, F. Molnar, W. Wriggers, and K. Schulten, Steered molecular dynamics, in *Computational Molecular Dynamics: Challenges, Methods, Ideas, Lecture Notes in Computational Science and Engineering*, edited by P. Deuflhard, J. Hermans, B.

Leimkuhler, A. E. Mark S. Reich, and R. D. Skeel, Vol. 4 (Springer, Berlin, 1999), pp. 39–65.

[10] E. Evans and K. Ritchie, Dynamic strength of molecular adhesion bonds, Biophys. J. **72**, 1541 (1997).

[11] W. Humphrey, A. Dalke, and K. Schulten, Sartorius products, J. Mol. Graph. **14**, 33 (1996).

[12] R. L. Baldwin, α-Helix formation by peptides of defined sequence, Biophys. Chem. **55**, 127 (1995).

[13] J. C. Phillips, D. J. Hardy, J. D. C. Maia, J. E. Stone, J. V. Ribeiro, R. C. Bernardi, R. Buch, G. Fiorin, J. Hénin, W. Jiang *et al.*, Scalable molecular dynamics on CPU and GPU architectures with NAMD, J. Chem. Phys. **153**, 044130 (2020).

[14] A. D. MacKerell, Jr., D. Bashford, M. Bellott, R. L. Dunbrack, Jr., J. D. Evanseck, M. J. Field, S. Fischer, J. Gao, H. Guo, S. Ha *et al.*, All-atom empirical potential for molecular modeling and dynamics studies of proteins, J. Phys. Chem. B **102**, 3586 (1998).

[15] R. B. Best, X. Zhu, J. Shim, P. E. M. Lopes, J. Mittal, M. Feig, and A. D. MacKerell, Optimization of the additive CHARMM all-atom protein force field targeting improved sampling of the backbone φ, ψ and side-chain $X1$ and $X2$ dihedral angles, J. Chem. Theory Comput. **8**, 3257 (2012).

[16] S. Takeda, A. Ptak, C. Nakamura, J. Miyake, M. Kageshima, S. P. Jarvis, and H. Tokumoto, Measurement of the length of the α helical section of a peptide directly using atomic force microscopy, Chem. Pharm. Bull. **49**, 1512 (2001).

[17] S. Takeda, A. Ptak, M. Kageshima, H. Tokumoto, C. Nakamura, and J. Miyake, Unfolding process of a single peptide molecule on a substrate was investigated by atomic force microscope, Surf. Sci. **532-535**, 244 (2003).

[18] See Supplemental Material at http://link.aps.org/supplemental/10.1103/PhysRevA.106.062803 for details on the simulation protocol, the unbinding force of a single hydrogen bond including characteristics and distribution, and analysis of α-helical structure in the peptide model.

[19] J. Dąbrowski, W. Nowak, and A. Ptak, How strong are hydrogen bonds in the peptide model? Phys. Chem. Chem. Phys. **22**, 1392 (2020).

[20] G. Bell, Models for the specific adhesion of cells to cells, Science **200**, 618 (1978).

[21] O. K. Dudko, G. Hummer, and A. Szabo, Intrinsic Rates and Activation Free Energies from Single-Molecule Pulling Experiments, Phys. Rev. Lett. **96**, 108101 (2006).

[22] G. A. Jeffrey and W. Saenger, *Hydrogen Bonding in Biological Structures* (Springer, Berlin, 1991).

[23] S. Y. Sheu, D. Y. Yang, H. L. Selzle, and E. W. Schlag, Energetics of hydrogen bonds in peptides, Proc. Natl. Acad. Sci. USA **100**, 12683 (2003).

[24] M. C. Baxa, E. J. Haddadian, J. M. Jumper, K. F. Freed, and T. R. Sosnick, Loss of conformational entropy in protein folding calculated using realistic ensembles and its implications for NMR-based calculations, Proc. Natl. Acad. Sci. USA **111**, 15396 (2014).